

# Analysis on Electric Field Based on Three Dimensional Atmospheric Electric Field Apparatus

Hong-yan Xing<sup>†</sup>, Gui-xian He<sup>\*</sup> and Xin-yuan Ji<sup>\*\*</sup>

**Abstract** – As a key component of lightning location system (LLS) for lightning warning, the atmospheric electric field measuring is required to have high accuracy. The Conventional methods of the existent electric field measurement meter can only detect the vertical component of the atmospheric electric field, which cannot acquire the realistic electric field in the thunderstorm. This paper proposed a three dimensional (3D) electric field system for atmospheric electric field measurement, which is capable of three orthogonal directions in X, Y, Z, measuring. By analyzing the relationship between the electric field and the relative permittivity of ground surface, the permittivity is calculated, and an efficiency 3D measurement model is derived. On this basis, a three-dimensional electric field sensor and a permittivity sensor are adopted to detect the spatial electric field. Moreover, the elevation and azimuth of the detected target are calculated, which reveal the location information of the target. Experimental results show that the proposed 3D electric field meter has satisfactory sensitivity to the three components of electric field. Additionally, several observation results in the fair and thunderstorm weather have been presented.

**Keywords:** Three dimension electric field, Permittivity sensor, Lightning, Electric field analysis.

## 1. Introduction

Monitoring of the atmosphere electric field is an essential part of lightning warming [1-2]. In recent years, atmospheric electric field measuring plays a more and more important role in many industrial and scientific areas, such as aerospace, meteorological, power grid and so on [3-4]. With the increasing use of electric equipment, the probability of electric system being destroyed by lightning electromagnetic pulse increases accordingly. Therefore, lightning detection has been a crucial problem in modern society. When the thundercloud is closing, the atmospheric electric field inside and outside the thundercloud changes violently, which can be used to predicted the lightning occurrences [5]. The atmospheric electric field measurement meter, as a conventional diagnostic tool, has been widely used in electric field detecting.

Many researches have been carried out to find out the charge center in a thunderstorm and to determine the structure of lightning by detecting the electric field with field mill type electric field meter, which can only detect the vertical electric field [6-7]. However, Due to the complexity of the electric field in the thunderstorm, the atmospheric electric field is affected by the charge distribution in the

cloud, which changes with the clouds changes [8]. So, there will be an existence of horizontal components of the electric field other than the vertical component. This has been well highlighted in Ref [9-11] and elsewhere. Therefore, it is important to investigate the 3D electric field components in thundercloud to propose more realistic atmospheric electric field. Up to now, many investigators have focused on the research of the horizontal components of the electric field. For example, Kamra *et al.* [12] developed a spherical electric field meter to measure the electric field vector at 1m above the ground. And later, Kamra *et al.* [13] extended their study on the spherical field meter with Maxwell's current density, which can find out the location of charge center and the charge destroy in a thunderstorm. Tantisattayakul *et al.* [14] developed a hybrid electric field meter to measure the vertical and horizontal electric fields in thunderstorm. Bateman *et al.* [15] discussed the application of the aircraft-based rotating-vane-style electric field mills in NASA's Marshall Space Flight Center. The mills were installed in the different positions of the aircraft, and then Mach *et al.* [16] calculated the relationship between the electric field measured at the aircraft and the external vector electric field through a calibration technique. Katsuki *et al.* [17] focused on the electro-optic probe for three-axis electric field measurement. However, those studies usually have complex fabrication process, big volumes and especially high cost.

Zheng [18] introduced spatial three dimensional electric filed measuring system based on L-band meteorological radar for aerial electric field measurement. [19] reported a 3D electric measuring method based on coplanar decoupling

<sup>†</sup> Corresponding Author: Collaborative Innovation Center on Forecast and Evaluation of Meteorological Disasters, Nanjing University of Information Science & Technology, China. (xinghy@njust.edu.cn.)

<sup>\*</sup> Key Laboratory for Aerosol-Cloud-Precipitation of China Meteorological Administration, Nanjing University of Information Science & Technology, China.(hgxx251@163.com)

<sup>\*\*</sup> Nanjing University of Information Science & Technology, China.

Received: September 7, 2017; Accepted: May 18, 2018

structure to deal with the issue of coupling in three components of electric field. Wang [20] presented a novel X-Y dual axis sensitive sensor for static electric field measurement, which is capable of two-dimensional electric field sensing.

These scholars further improved the 2D and 3D electric field measuring instruments from the aspects of materials and structures, which solved the problems of the three-dimensional electric field measurement in the air and the coupling of the electric field components between the existing electric field sensors. However, their study did not consider the influence of the dielectric constant on the measurement of the electric field. Because of the good conductivity of the earth, researchers usually regard the earth as a conductor. It is considered that the electric field near the ground is perpendicular to the ground surface. However, in reality, the surface layer of the earth is a complex structure, which composed of different components such as soil, rock, and water. So it has a certain dielectric constant and dielectric properties on the surface layer. The electric field near the ground will be tilted, which result in a horizontal component. Therefore, neglect its dielectric properties when measuring 3D electric fields will affect the accuracy of the results. Till now, no such researches relevant to 3D electric field meter with permittivity measurement or azimuth information of the thunderstorm detected by electric mills have been reported. The three-dimensional electric field sensor adopts the principle of electrostatic induction. Three sets of orthogonal electrostatic induction units are arranged on the outside of the sensor, and the three-dimensional electric field is measured by forming a differential signal through the shielding and exposure of the three groups of sensing units.

In this paper, in an attempt to attain more realistic atmospheric electric field, considering the influence of the permittivity, a 3D electric field system is proposed. The permittivity sensor is used in this work. The three electric component of X, Y, Z, axis are measured by this device. In addition, the elevation and azimuth of the target are carried out.

## 2. Principle Analysis of Three Dimensional Electric Field Measurement

### 2.1 Three dimensional electric field model

In this section, the principle of 3D electric field measurement model in a thunderstorm is presented in Fig. 1. As shown in Fig. 1, A, B represent the observation site and thunderclouds respectively.  $\alpha$  is the azimuth angle of the thunderclouds.  $\gamma$  represents the elevation angle of the thunderclouds. From Fig. 1, it can be seen that the aerial electric field  $E$  is a three-dimensional vector, which can be decomposed into  $E_x$ ,  $E_y$ ,  $E_z$  three components orthogonally. The relationship of the three electric components is given

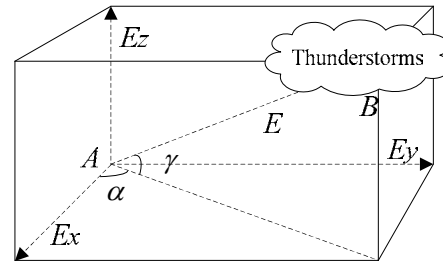


**Fig. 1.** 3D electric field model

as follows:

$$E = E_x + E_y + E_z \quad (1)$$

### 2.2 Method analysis

In order to establish the electric field distribution generated by the net charge in the air, the thunderstorm cloud and the earth are regarded as a point charge and an infinite dielectric plane respectively. According to the mirror method theory, it can be assumed that the electric field generated by the point charge which is at any point of the region, is generated by the point charge  $q$  and its mirror charge  $q_1$ . Therefore, the potential distribution  $\phi_1$  of the thunderstorm at the ground observation station can be obtained by Eq. (2)

$$\phi_1 = \frac{1}{4\pi\epsilon_1} \left[ \frac{q}{\sqrt{x^2 + y^2 + (z-H)^2}} - \frac{\epsilon_2 - \epsilon_1}{\epsilon_2 + \epsilon_1} \frac{q_1}{\sqrt{x^2 + y^2 + (z+H)^2}} \right] \quad (2)$$

Where  $\epsilon_1$  is the permittivity of the air;  $\epsilon_2$  is the permittivity of the Dielectric;  $x$ ,  $y$ ,  $z$  represent the coordinates of the target thunderstorm;  $H$  is the altitude of the observe-station.

Then the electric field components of  $E_x$ ,  $E_y$ ,  $E_z$  will be calculated by (3)-(5) as follows:

$$E_x = \frac{\partial \phi_1}{\partial x} = \frac{-qx}{4\pi\epsilon_1} \left\{ [x^2 + y^2 + (z-H)^2]^{-3/2} - \frac{\epsilon_2 - \epsilon_1}{\epsilon_2 + \epsilon_1} [x^2 + y^2 + (z+H)^2]^{-3/2} \right\} \quad (3)$$

$$E_y = \frac{\partial \phi_1}{\partial y} = \frac{-qy}{4\pi\epsilon_1} \left\{ [x^2 + y^2 + (z-H)^2]^{-3/2} - \frac{\epsilon_2 - \epsilon_1}{\epsilon_2 + \epsilon_1} [x^2 + y^2 + (z+H)^2]^{-3/2} \right\} \quad (4)$$

$$E_z = \frac{\partial \phi_1}{\partial z} = \frac{-q}{4\pi\epsilon_1} \left\{ (z-H)[x^2 + y^2 + (z-H)^2]^{-3/2} - \frac{\epsilon_2 - \epsilon_1}{\epsilon_2 + \epsilon_1} (z+H)[x^2 + y^2 + (z+H)^2]^{-3/2} \right\} \quad (5)$$

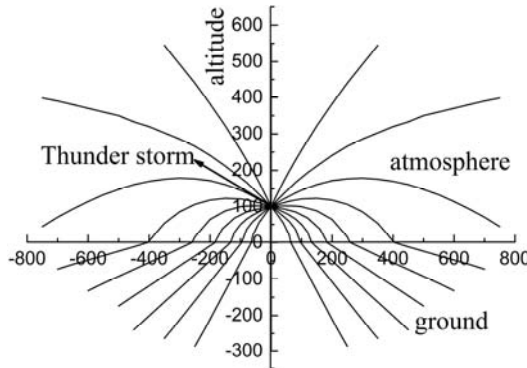


**Fig. 2.** Electric field distribution of aerial charge

According to the vector relationship, the azimuth angle  $\alpha$  and the elevation angle  $\gamma$  can be determined by (6)-(7), respectively.

$$\operatorname{tg} \alpha = \frac{E_y}{E_x} \quad (6)$$

$$\operatorname{tg} \gamma = \frac{z}{\sqrt{x^2 + y^2}} = \frac{\varepsilon_1 E_z}{\varepsilon_2 \sqrt{E_x^2 + E_y^2}} \quad (7)$$

In order to verify the influence of the dielectric constant on the electric field near the ground surface, an air thunderstorm cloud and ground model was established. The thunderstorm cloud is equivalent to a point charge coordinate of (0,100). The earth is equivalent to an infinitely large dielectric plane. The dielectric constant of the air  $\varepsilon_1$  is set to 1; the permittivity of the earth  $\varepsilon_2$  is set to 5. The distribution curve of the thunderstorm cloud electric field above and below the ground is solved by the image method. The result is shown in the Fig. 2.

From Fig. 2, we can clearly see that the electric field of the thunderstorm cloud presents a certain angle with the earth's surface when considering the permittivity of the ground. At the same time, the electric field below the surface is ray-like and points to the air charge. Therefore, when we measure the ground electric field, the real situation of the electric field can be measured more accurately by considering the influence of the permittivity of the earth.

### 3. Structure Design

To ameliorate the measurement accuracy of atmospheric electric field, we combine the 3D electric field measurement unit with permittivity measurement unit to obtain a fusion framework. The schematic diagram is shown in Fig.3. As shown in Fig.3, the two sensors convert the physical signals into electrical signals. And then through signal conditioning, photoelectric conversion, we convert the electrical signals to the digital signals, which are finally sent to the main control system for acquisition and

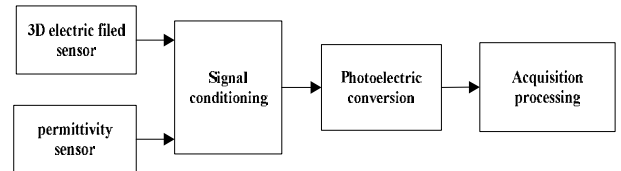


**Fig. 3.** Proposed framework of 3D electric field instrument

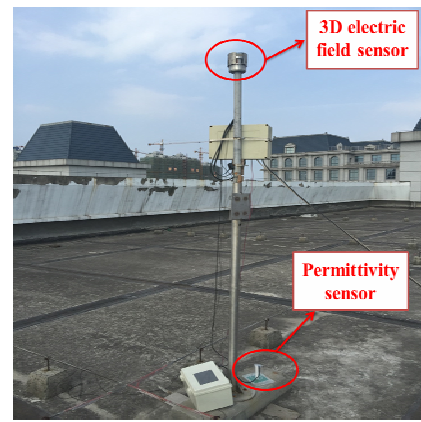


**Fig. 4.** 3D electric field measurement system in NUIST station

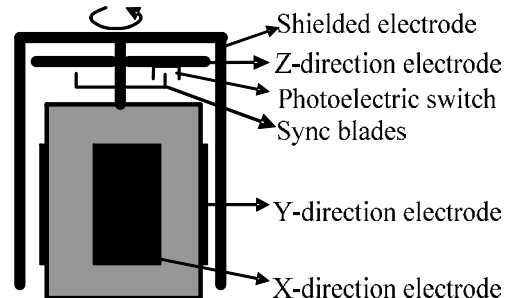


**Fig. 5.** Outline of the 3D electric field unit

processing. The 3D atmospheric electric field measurement meter designed and fabricated by us is presented in Fig.4, which is located in NUIST station (32°12'N, 118°42'E, 22.4 m above mean sea level).

#### 3.1 3D electric field measurement unit

The outline of the 3D electric field measured unit, which is designed based on the electrostatic induction principle, is illustrated in Fig. 5. The 3D electric field measurement unit mainly consists of a Rotating Electrode, a Fixed Electrode, a Photoelectric Switch and the Sync blades. The Rotating Electrode includes the shielded electrode and a Motor, and the Fixed Electrode mainly includes the x, y, z direction electrodes. The x and y direction contain a set of sensing electrodes, which is oppositely placed. The x, y, z direction electrodes are periodically shielded from the environment electric field  $E$  by the shielded electrode

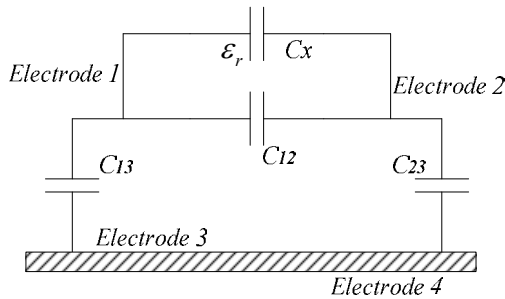


**Fig. 6.** Equivalent circuit of permittivity measurement

rotating around the vertical axis.  $q_x$ ,  $q_y$ ,  $q_z$  are the charge induced on the  $x$ ,  $y$ ,  $z$  direction electrodes due to  $E$ .  $i_x$ ,  $i_y$ ,  $i_z$  are the alternating current signal created by the change of  $\Delta q_x$ ,  $\Delta q_y$ ,  $\Delta q_z$ , respectively. And later, we make use of the square wave generated by the photoelectric switch to carry out phase-detection and acquire the voltage signals which are proportional to three components of the electric field respectively.

### 3.2 Permittivity measurement unit

Aiming at solving the influence of the permittivity when measuring the electric field as shown in Eqs. (3)-(5), a permittivity measurement unit was put forward to acquire the material's permittivity. The equivalent circuit of the permittivity measurement system is shown in Fig. 6. The principle of the system is the changing of the capacitance with different filling medium between electrodes. As shown in Fig. 6, the system mainly includes the coplanar capacity sensor with 4 electrodes. Electrode1 and Electrode 2 are the measurement electrodes. Electrode 3 and electrode 4 are the shielded electrodes, which are connected to the ground in order to shield the interference of the environment electric field. The capacitance  $C_x$  is the measuring capacitance between the electrode1 and 2. The difference  $\Delta C$  of the capacitance  $C_x$  and  $C_{air}$  is the Linear function of the measuring material's permittivity [21]. The values of the capacitance  $C_{12}$ ,  $C_{13}$ ,  $C_{23}$  are fixed which can be eliminate during measuring. So, the permittivity can be obtained as follows

$$\varepsilon_r = \frac{\Delta C}{C_{air}} + 1 \quad (8)$$

Where  $\varepsilon_r$ : permittivity.

## 4. Experimental Results and Discussion

### 4.1 Observation results in fair weather

The 3D electric field measurement meter was installed on the roof of the electrical engineering building, NUIST station (as shown in Fig. 4), which was approximately

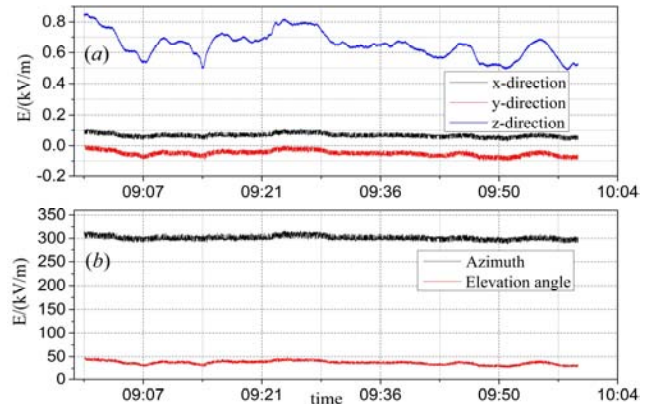


**Fig. 7.** Observation results of 3D electric field system (2017/07/25): (a) 3D electric field on a clear day; (b) Change of Azimuth and Elevation angle on a clear day

**Table 1.** Analysis results of atmospheric electric field in fair weather

Source	NUIST		REF [22]	
	AVG	STD	AVG	STD
$E_x$	0.0682	0.0153	---	---
$E_y$	-0.049	0.203	---	---
$E_z$	0.6513	0.0831	0.637	0.073

22.5m above the mean sea level. The values of  $E_x$ ,  $E_y$ ,  $E_z$  are recorded on the computer for every second, and the elevation and azimuth angles are calculated at the same time. Fig. 7 shows a part of the observation data in a fair weather. In our study, we have defined the North as originating direction ( $0^\circ$ ) and defined the South as  $180^\circ$ . As shown in Fig. 7 (a), the value of the  $E_x$  is much bigger than those electric field value in horizontal direction ( $E_y$ ,  $E_z$ ). We can also see that  $E_x$ ,  $E_z$  indicate the positive polarity, while  $E_y$  is negative polarity in this observation. The statistical calculation on the electric field of Fig. 7 (a) is listed in Table 1. According to the statistical results, the average (AVG) and the standard deviation (STD) of the atmospheric electric field (EF) in vertical direction ( $0.6513\text{KV m}^{-1}$ ,  $0.0831$ ) are similar to those ( $0.637\text{KV m}^{-1}$ ,  $0.073$ ) observed in Ref [22] by conventional electric field instruments. Fig. 7 (b) typified the trend of the elevation and azimuth angles in a clear day, which clearly show that the fluctuation range of the angles is small.

### 4.2 Observation results in thunderstorm weather

Shown in Figs. 8 and 9 are time series plots of atmospheric electric field data observed in thunderstorm weathers. As displayed in Fig. 9, during the thunderstorm, the fluctuation range of the  $E_x$ ,  $E_y$ ,  $E_z$  obtained from the 3D electric field mill are significantly larger than those on a fair day. From Fig. 8 (a), we can clearly see that the changing trends of vertical and vertical components of electric field are basically consistent during 4:48-6:20.

However, the amplitude of  $E_z$  is much larger than  $E_x$  and  $E_y$ . Noting that during the time 4:48-6:20, the electric field has several polarity reversals with the obvious change in elevation and azimuth angles. This is probably due to the discharge activities in the thunderstorms.

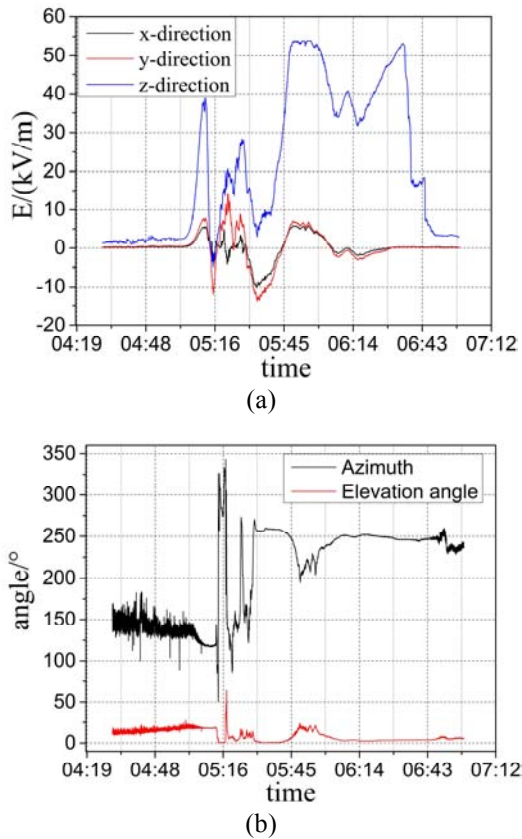


**Fig. 8.** Observation results of 3D electric field system (2016/05/05): (a) 3D electric field in thunderstorm weather; (b) Change of Azimuth and Elevation angle in thunderstorm weather

Fig. 9 shows another instance of observed data in thunderstorm weather. As illustrated in the waveforms of  $x$ ,  $y$ ,  $z$  direction, the 3D electric field meter could detect the rapid electric field changes caused by lightning discharge activities in the thunderstorm. The Azimuth and Elevation angles are given as the azimuth information of the thunderstorm, which defined 0° as the north and 90° as the eastward. As seen in Fig. 9 (a), there are peak values of  $E_z$  at around 15:27 and 15:38. And Fig. 9 (b) shows that the elevation angles are around 70° at the time 15:27 and 15:38. And thus we can estimate that there is possibility of an existence of a thunderstorm above the apparatus at that time.

In order to confirm the result, the radar echoes from 14:57 to 15:39 which correspond to this data are shown in Fig. 10. The red point in the maps is the observation point in NUIST station. From Fig. 10 (a) and (b), we can see that the thunderstorm is at the direction of northwest to northeast range at 14:57, while the direction of the thunderstorm changes to the northeast at around 15:09. Meanwhile, we can know from Fig. 9 (b) that there is an inversion of the azimuth angle from around 300°(northwest direction) to around 40°(northeast direction) at around 15:09, with which agree well with the changes of the radar echoes (a)-(b).

The values of  $E_z$  reached the peak value at around 15:27, while the values of  $E_x$ ,  $E_y$  are small as shown in Fig. 9 (a), from which we can assume that there had been electric charge accumulated in the thunderstorm above the NUIST station. And from Fig. 10 (c), we can see that the thunderstorm was above the NUIST station and the echo intensity exceeded 45dbz at that time, which was consistent with the result obtained by the 3D electric field meter. At the time around 15:39, there were negative peak values of  $E_x$ ,  $E_y$ ,  $E_z$ . The fluctuation range of the azimuth and elevation angles at 15:39 were significantly larger than that time 15:27, from which we can estimate

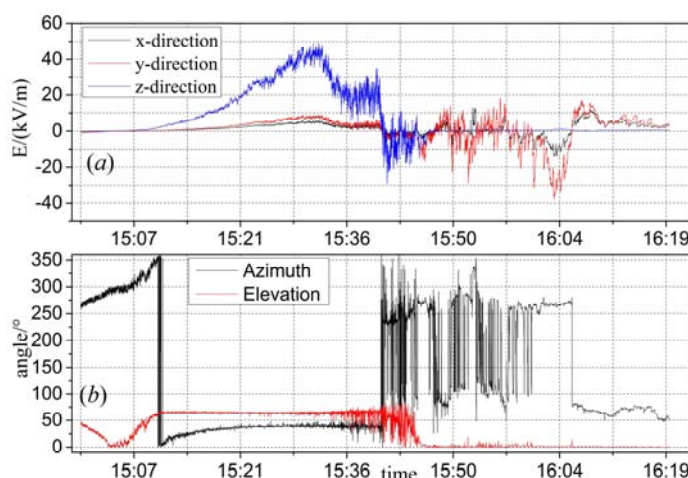


**Fig. 9.** Observation results of 3D electric field system (2017/08/05): (a) 3D electric field in thunderstorm weather; (b) Change of Azimuth and Elevation angle in thunderstorm weather

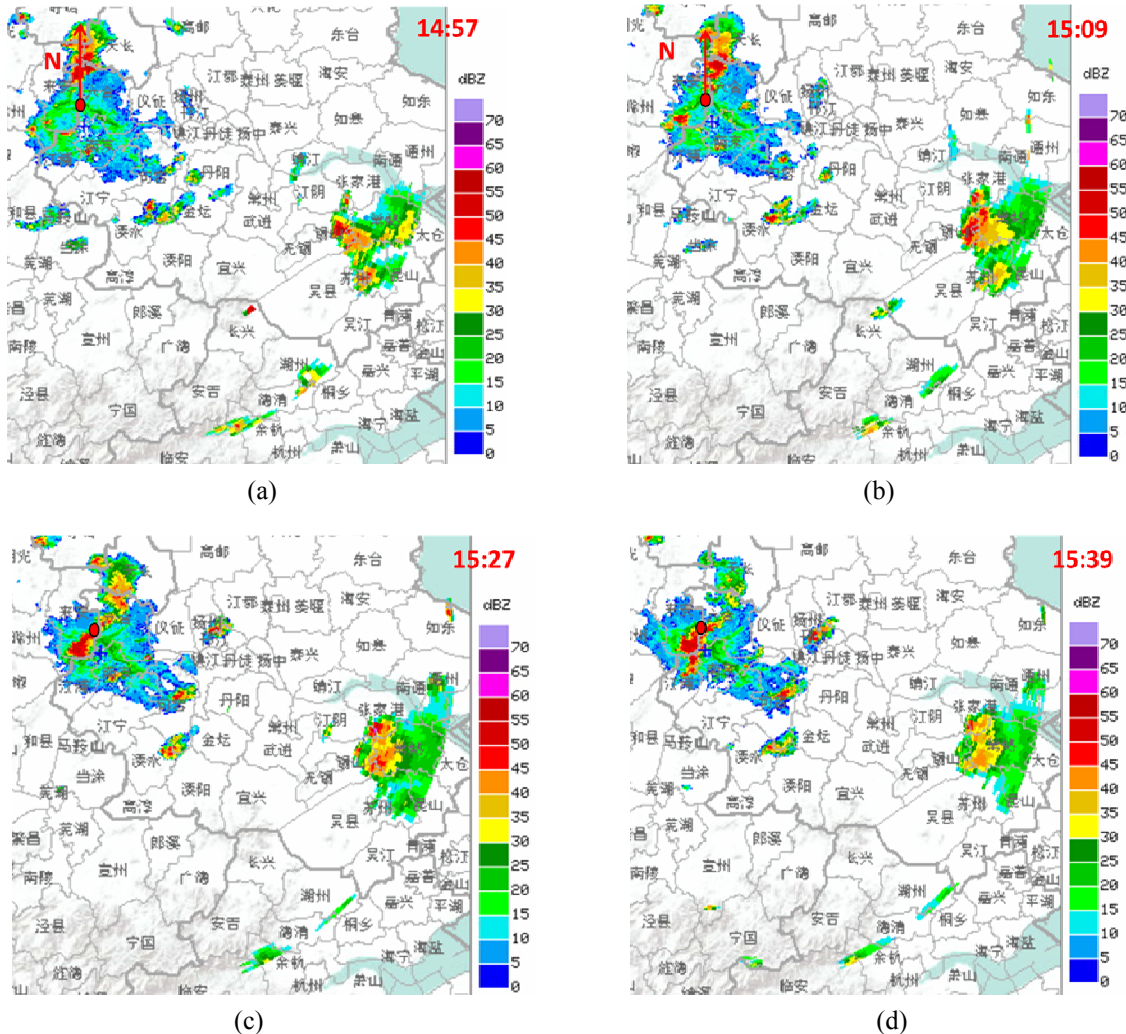


**Fig. 10.** The radar echoes from 14:57 to 15:39 in thunderstorm weather

that there are severe lightning discharge activities in the thunderstorm. Fig. 10 (d) shows that the center of the thunderstorm was near the apparatus at 15:27. And the large fluctuation of the angles is probably due to the charge structure of the thundercloud.

## 5. Conclusion

In this paper, a three dimensional electric field meter was demonstrated for high precision electric measurement. In order to study the influence of the permittivity on the electric measurement, a permittivity Measuring unit was adopted in the system. Later, experiments were done on the NUIST station with our 3D electric field apparatus. The experiment results show that the meter has the satisfactory response to the three components of the environment electric field. Moreover, the elevation and azimuth estimation information of the thundercloud can be obtained by using the electric field meter. Using the proposed methodology, the elevation and azimuth information of the

thunderstorm cloud can be well obtained. This apparatus improves the accuracy of the thunderstorm cloud electric field measurement to a certain extent, and ensures the quality of atmospheric electric field monitoring data. At the same time, it also provides a basis for subsequent multi-station positioning of thunderstorms and automatic monitoring and early warning of thunderstorms through cluster analysis in the future. Therefore, this method is expected to help enhance the accuracy and reliability of lightning automated warming system.

## Acknowledgements

The work is supported by the National Natural Science Foundation of China under grant 61671248 and 41605121; The Priority Academic Program Development of Jiangsu Higher Education Institutions(PAPD); Major Projects of Natural Science Research in Universities of Jiangsu Province (15KJA460008).

## References

- [1] J. Montanya, J. Bergas and B Hermoso, "Electric field measurements at ground level as a basis for lightning hazard warning," *Journal of Electrostatics*, vol. 60, no. 2, pp. 241-246, 2004.
- [2] M.A.D.S. Ferro, J. Yamasaki, D.R.M. Pimentel and K.P. Naccarato, "Lightning risk warnings based on atmospheric electric field measurements in Brazil," *Journal of Aerospace Technology and Management*, vol. 3, no. 3, pp. 301-310, 2011.
- [3] Q. Zeng, Z. Wang, F. Guo, M. Feng, S. Zhou, *et al*, "The application of lightning forecasting based on surface electrostatic field observations and radar data," *Journal of Electrostatics*, vol. 71, no. 1, pp. 6-13, 2013.
- [4] D.A. Nag, V.A. Rakov, D. Tsakiris, J.S. Howard, C.J. Biagi, *et al*, "Characteristics of the initial rising portion of near and far lightning return stroke electric field waveforms," *Atmospheric Research*, vol. 117, no. 12, pp. 71-77, 2012.
- [5] D. Aranguren, J. Montanya, G. Soláa, V. Marcha, D. Romeroa and H. Torresb, "On the lightning hazard warning using electrostatic field: Analysis of summer thunderstorms in Spain," *Journal of Electrostatics*, vol. 67, no. 2, pp. 507-512, 2009.
- [6] C. Schumann, R.B. Silva, W. Schulz, "Electric fields changes produced by positives cloud-to-ground lightning flashes," *Journal of Atmospheric and Solar-Terrestrial Physics*, vol. 92, no. 1, pp. 37-42, 2013.
- [7] A. Fort, M. Mugnaini, V. Vignoli, S. Rocchi, F. Perini, J. Monari, M. Schiaffino and F. Fiocchi, "Design, modeling, and test of a system for atmospheric electric field measurement," *IEEE Transactions on Instrumentation and Measurement*, vol. 60, no. 8, pp. 2778-2785, 2011.
- [8] M. Stolzeburg, T.C. Marshall, *et al.*, Lightning: Principles, Instruments and Applications[M]. Germany, Springer Science Business Media, 2009, Chapter 3.
- [9] P. Baranski, M. Loboda, J. Wiszniewski and Marek Morawski, "Evaluation of multiple ground flash charge structure from electric field measurements using the local lightning detection network in the region of Warsaw," *Atmospheric Research*, vol. 117, pp. 99-110, 2012.
- [10] J. Lopez, E. Perez, J. Herrera and D. Aranguren, "Thunderstorm warning alarms methodology using electric field mills and lightning location networks in mountainous regions," *International Conference on Lightning Protection*, 2012, pp. 1-6.
- [11] R. Vishnu, V. A. Kumar, T. S. Sreekanth, V. N. S. Symon, S. M. Das and G. M. Kumar, "Formation of thunderclouds in a region of high lightning incidence, inferred from AWS, ceilometer and an electric field mill," *Asia-pacific International Conference on Lightning*, 2011, pp. 135-139.
- [12] A. K. Kamra, "Spherical field meter for measurement of the electric field vector," *Review of Scientific Instruments*, vol. 10, pp. 1401-1406, 1983.
- [13] M. Ravichandran, A.K. Kamra, "A new technique to determine the lightning charge location from the electric field vector measurements," *Journal of Atmospheric and Solar-Terrestrial Physics*, vol. 66, pp. 349-362, 2004.
- [14] T. Tantisattayakul, K. Masugata, I. Kitamura and K. Kontani, "Development of the Hybrid Electric Field Meter for Simultaneous Measuring of Vertical and Horizontal Electric Fields of the Thundercloud," *IEEE Transactions on electromagnetic compatibility*, vol. 2, pp. 435-438, 2006.
- [15] M. G. Bateman, M. F. Stewart, R.J. Blakeslee, S.J. Podgorny, H.J. Christian, "A low-noise, microprocessor-controlled, internally digitizing rotating-vane electric field mill for airborne platforms," *Journal of Atmospheric and Oceanic Technology*, vol. 24, no. 7, pp. 1245-1255, 2007.
- [16] D. M. Mach, W. J. Koshak, "General matrix inversion technique for the calibration of electric field sensor arrays on aircraft platforms," *Journal of Atmospheric and Oceanic Technology*, vol. 24, no. 9, pp. 1576-1587, 2007.
- [17] K. Kiminami, T. Iyama, T. Onishi, "A three-axis electro-optic probe for specific absorption rate measurement," *Proceedings of the XXIX General Assembly of the International Union of Radio Science (URSI)*, KAE, 2008, pp. 993-996.
- [18] F.J. Zheng, S.H. Xia, "Spatial Three Dimensional Electric Field Measuring System Basing on L-Band Meteorological Radar," *Journal of Electronics & Information Technology*, vol. 34, no. 7, pp. 1637-1641, 2012.
- [19] X.L. Wen, C.R. Peng, D.M. Fang, *et al.*, "Measuring Method of Three Dimensional Atmospheric Electric Field Based on Coplanar Decoupling Structure," *Journal of Electronics & Information Technology*, vol. 36, no. 10, pp. 2504-2508, 2014.
- [20] Y. Wang, D. Fang, K. Feng, *et al.*, "A novel micro electric field sensor with X-Y dual axis sensitive differential structure," *Sensors & Actuators A Physical*, vol. 229, pp. 1-7, 2015.
- [21] X.Y. Ji, H.Y. Xing, W. Xu, "Design of relative dielectric constant real-time monitoring system," *Instrument Technique and Sensor*, vol. 2, pp. 42-44, 2016.
- [22] H.J. Wan, G.H. Wei, Y.Z. Cui, Y.Z. Chen, "Influence factor analysis of atmospheric electric field monitoring near ground under different weather conditions," *7th International Conference on Applied Electrostatics (ICAES-2012)*, 2012.



**Hong-yan Xing** He received B. Sc. from Taiyuan University of Technology in 1983, M. Sc. From Jilin University in 1990 and Ph. D. from Xi'an Jiaotong University in 2003, respectively. Now he is a professor in Nanjing University of Information Science & Technology. His main research interests are design and metering of meteorological instruments, signal detection and processing and lightning protection.



**Gui-xian He** He received B. Sc. from Nanjing University of Information Science & Technology in 2015. He is a M.Sc. candidate in Nanjing University of Information Science & Technology now. His present research interest includes instrumentation technology, lightning protection.



**Xin-yuan Ji** He is currently a doctoral student in the school of Atmospheric Physics, Nanjing University of Information Science & Technology, Nanjing, China. He obtained his master degree from Nanjing Normal University in 2005. His current research interest is meteorological instrument design.